Transactions of the Materials Research Society of Japan 33[3] 541-545 (2008)

Slow Neutron Optics

Hirohiko M. Shimizu
High Energy Accelerator Research Organization (KEK), 1-1 Oho, Tsukuba, Ibaraki 305-0801, Japan
Fax: 81-29-864-3202, e-mail: hirohiko.shimizu@kek.jp

We survey the current status of reflective neutron optical devices, compound refractive and magnetic ones for enhancing the effectiveness of the beam utilization to extract physics information of samples.
Key words: neutron beam, neutron optics

1. INTRODUCTION

Neutron is a neutral hadron, which decays with the mean lifetime of about 15 minutes. The long lifetime enables us to decelerate to low kinetic energy regions at the level of the thermal motion of atoms in materials. The neutron provides a unique opportunity to study the position of light atoms and the dynamics in materials, which is complementary to photon probes such as X-rays. However, the neutron beam luminosity is low since we must use the low energy neutrons evaporated from the surface of the moderator. The effective size of the moderator is about 10 cm, which is determined from the ratio of scattering cross section and absorption cross section. The low luminosity of neutron beam limits the general application to various samples, which are usually unavailable in large amount. A direct solution to overcome the situation is to increase the beam intensity. The increase of source intensity is being realized by constructing new spallation sources such as the Spallation Neutron Source (SNS) in US and the Japan Proton Accelerator Research Complex (J-PARC) in Japan[1]. Another independent approach is to apply advanced optical components to enhance the efficacy of the beam utilization. The beam efficacy has been very low since the beam emittance is very large. In the last decade, the neutron optics has been remarkably improved following the breakthrough of neutron optical devices.

2. NEUTRON REFLECTIVE OPTICS

The interaction of neutrons on material surface can be approximately described by using the effective potential U, which is given as

$$U = \frac{2\pi\hbar^2}{m_n} bN, \tag{1}$$

where b is the neutron scattering length, N the nuclear number density of the material and m_n the neutron mass. Neutrons are reflected and refracted on the surface of materials due to the difference of the effective potential on the interface of materials. The incident neutron is reflected and refracted on the interface in the Fig.1 as

$$\frac{\sin\theta}{\sin\Theta} = \sqrt{1 - \frac{m_n}{2\pi^2\hbar^2}(U_2 - U_1)}\ , \tag{2}$$

where U_1 and U_2 are the effective potentials in the region 1 and 2.

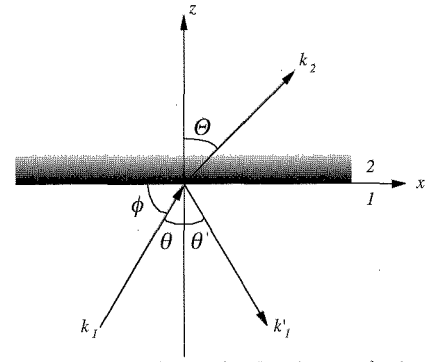

Fig.1. Neutron reflection and refraction on the interface of materials.

The reflectivity R is given as

$$R = \left| \frac{1 - \sqrt{1 - (\phi_c/\phi)^2}}{1 + \sqrt{1 - (\phi_c/\phi)^2}} \right|^2, \tag{3}$$

where ϕ_c is defined as

$$\phi_c = \lambda\sqrt{\frac{bN}{\pi}}, \tag{4}$$

where λ is the neutron wavelength. The ϕ_c is referred to as the critical angle of total reflection since neutrons are totally reflected for $\phi < \phi_c$ if b is a positive real number.

The reflectivity can be increased beyond the critical angle by using the diffraction in a stack of artificial pair layers comprising of materials, which have different effective potentials. The reflectivity can be continuously extended beyond the critical angle by adjusting the thickness of the pair layers as schematically shown in Fig.2. The mirror coated with the multilayer for the continuous enhancement of the reflectivity beyond the critical angle is referred to as the supermirror. The performance of a supermirror can be characterized with the grazing angle and the reflectivity at the drop-edge of the reflectivity curve. The grazing angle at the drop-edge is commonly measured in the unit of the critical angle of

a natural nickel surface ($\phi_{c,Ni}/\lambda$=0.017 rad nm^{-1}), which is referred to as the m-value. The deposition technique must be carefully developed in the precise control of the thickness and uniformity of each layer in order to increase the m-value since the large grazing angle corresponds to thin pair layers. The largest m-value was m=4 in 1990's[2], which has been remarkably improved in the early 2000's after the successful fabrication of m=5 and m=6 supermirrors[3]. Large m-value supermirrors can be applied to bend neutron beams with large angles. We can bend neutrons of λ=0.4 nm by about 5 degrees using an m=6 supermirror.

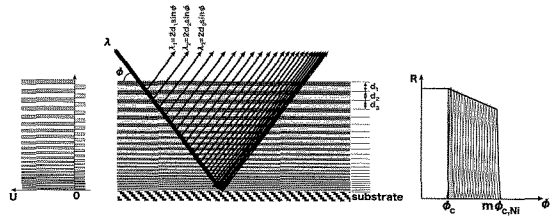

Fig.2. Schematic illustration of the layer structure of neutron supermirrors. The potential contrast in the multilayer is typically realized using nickel and titanium layers. The reflectivity beyond the critical angle of the substrate can be continuously increased according to the neutron diffraction in the multilayer.

Neutrons can be transported through neutron guides to neutron scattering instruments located remote from neutron sources. A neutron guide is a hollow duct, in most cases with a rectangular cross section, of which inner surfaces are neutron mirrors. We can increase the total number of neutrons delivered to the scattering instruments by employing large m-value supermirror guides since it is proportional to m^2 if we assume the reflectivity of the inner surface of the neutron guide is 100%.

Neutron supermirrors with magnetic material layers are capable of reflecting neutrons spin-selectively. The magnetic supermirror is a widely used as the neutron spin polarizer and analyzer. Large m-value magnetic supermirros are also under development in the range of m=4-5[4].

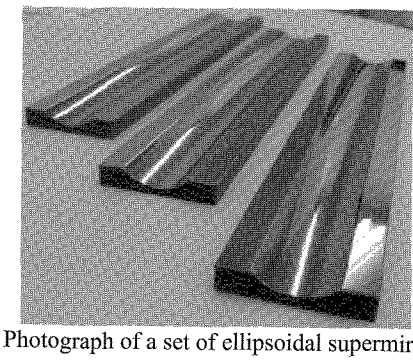

Fig.3. Photograph of a set of ellipsoidal supermirrors.

Neutron mirrors are also applied to focus neutron beams by approximating curved surfaces using mechanically bent mirrors or a mosaic of mirror pieces. In recent years, more accurate focusing has become available according to the successful application of the supermirror coating on to curved surfaces machined by the numerical control[5]. Fig.3 shows a set of ellipsoidal supermirrors[6].

3. NEUTRON REFRACTIVE OPTICS

Practical applications of neutron refractive optics has just begun in this decade. The advantage of the refractive optics is that the geometrical size is the real aperture and is larger compared with the reflective optics since only the grazing incident neutrons can be reflected. Additionally, refractive optics allows us to linearly configure the instrument on the beam axis. In this section, we review the compound refractive optics and magnetic optics. Both of them are wavelength dependent optics. The wavelength dependence is applicable to a crude spectroscopy, but it causes chromatic aberration in focusing polychromatic neutrons.

3.1 Compound refractive optics

Neutrons are refracted on material surfaces according to Eq.2. The refraction angle on the transmission through a prism shown in Fig.4 is given as

$$\sin\theta' = \sin(\theta+\beta)\cos\beta - \sqrt{\cos^2(\theta+\beta) - \frac{bN\lambda^2}{\pi}}\sin\beta \quad (5)$$

$$\underset{\theta\to 0}{\sim} \sin\theta + \frac{\phi_c^2}{2}\tan\beta$$

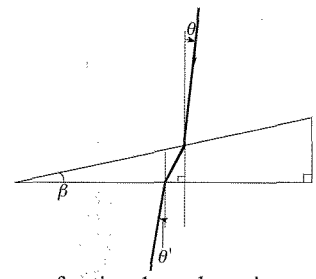

Fig.4. Neutron refraction through a prism.

The neutron optics based on the refraction on the surface of the material is referred to as the compound refractive optics. The application of the compound refractive optics became practical following the successful demonstration of the cold neutron beam focus and application to the small angle neutron scattering in focusing geometry[7,8].

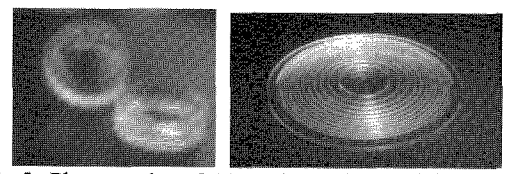

Fig.5. Photographs of MgF_2 lens pieces of biconcave shape (left) and Fresnel-shape (right).

The lens material should have larger scattering length with smaller absorption, which corresponds to maximize $|V/W|$, where $U = V - iW$. In addition, it should not have any significant small angle scattering. MgF_2 is the most commonly used material. The effective potential of MgF_2 is $U = (131 - 1.8\times10^{-4}i)$ neV and $\phi_c/\lambda = 0.013$ rad nm^{-1}. We show biconcave MgF_2 lens pieces and Fresnel-shape MgF_2 lens pieces in Fig.5 [9]. In both

cases, lens pieces are concave shape to focus neutrons since the positive real part of the effective potential corresponds to the refractive index smaller than unity as a result of Eq. (2).

The neutron trajectory is bent only on the lens surface. We can increase the total refraction angle of stacked Fresnel-shape lenses by increasing the number of lense pieces or by increasing the angle β of each lens piece. The total refraction angle in each case is given as

$$\theta_1 = \frac{L}{w\tan\beta_1}\frac{\phi_c^2}{2}\tan\beta_1 \sim \frac{\phi_c^2 L}{2w}, \qquad \theta_2 = \frac{\phi_c^2}{2}\tan\beta_2 \sim \frac{\phi_c^2 L}{2w}. \tag{6}$$

The total refraction angle is independent of the angle β for the same Fresnel pitch w and the total thickness L, which is limited by the requirement of the transmittance. Therefore, we can arbitrarily choose the angle β simply from the fabrication comfortableness.

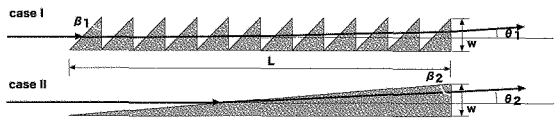

Fig.6. Illustration of two cases to increase the total refraction angle through compound refractive lenses.

A stack of thin Fresnel-shape lenses is being studied using the perfluoropolymer, which has the potential of $U = (117 - 3.7\times10^{-5} i)$ neV . We refer to the thin Fresnel-shape lens piece as the microprism. The refraction of the neutron beam has been successfully observed in the wavelength region of λ=0.1 nm using a stack of 500 pieces of 100μm-pitch microprisms[10].

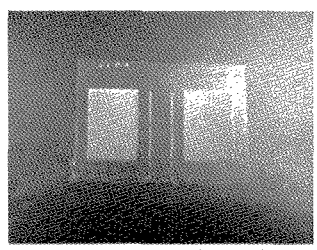

Fig.7. Photograph of a 100μm-pitch microprism made of a perfluoropolymer.

3.2 Magnetic optics

In this paper, we refer to a type of neutron optics using the acceleration of neutrons in inhomogeneous magnetic field as the magnetic optics. There is no parasitic scattering in magnetic optics and the beam trajectory can be accurately calculated since there is no material on the beam path.

The equation of motion of neutrons in an inhomogeneous magnetic field $\vec{B}$ can be approximated as

$$\frac{d^2\vec{r}}{dt^2} = \mp\alpha\nabla|\vec{B}|, \tag{7}$$

as long as the neutron spin is transported adiabatically, which corresponds to that the rotation of the local magnetic field seen by neutrons is sufficiently slow compared with the Larmor precession. The $\mp$ signs correspond to the cases the neutron spin is parallel and anti-parallel to the local magnetic field and $\alpha = \mu/m = 5.77$ T^{-1} m^2 s^{-2}. We take the z-axis as the beam axis, x-axis as the horizontal axis and y-axis as the vertical axis. We define a 2(n+1)-pole magnetic field as

$$|\vec{B}| = B_n(\rho/\rho_0)^n, \tag{8}$$

where $\rho^2=x^2+y^2$ and ρ_0 is the magnet aperture. We define

$$\omega^2 = \alpha\frac{nB_n}{\rho_0^2},\ \theta = \omega t,\ X = \frac{x}{\rho_0},\ Y = \frac{y}{\rho_0},\ \Xi = \frac{dX}{d\theta},\ H = \frac{dX}{d\theta}, \tag{9}$$

and obtain

$$\frac{d^2X}{d\theta^2} = \mp X\cdot\left(X^2+Y^2\right)^{\frac{n}{2}-1},\quad \frac{d^2Y}{d\theta^2} = \mp Y\cdot\left(X^2+Y^2\right)^{\frac{n}{2}-1}. \tag{10}$$

The spin-parallel and anti-parallel neutrons are attracted to and swept off the magnet axis, respectively, for all cases of $n\geq1$. The equation (10) implies that the beam shape is simply rotated on (X,Ξ) and (Y,H) planes if n=2 and differentially rotated in other cases. Therefore, a sextupole magnet (n=2) can focus monochromatic neutrons from a point source to a point image. On the other hand, quadrupole magnet (n=1) has the strongest spin-selectivity since the field gradient is distributed over the entire aperture, which can be used as the neutron polarizer.

The magnetic optics requires a strong multipole magnet since the neutron magnetic moment is about 2000 times smaller than the electron magnetic moment. Permanent multipole magnets with the Halbach-type pole configuration or the extended Halbach-type pole configuration are commonly used for the neutron magnetic optics. Figure 8 shows the examples of the realization of sextupole and quadrupole neutron magnetic optics[11-15].

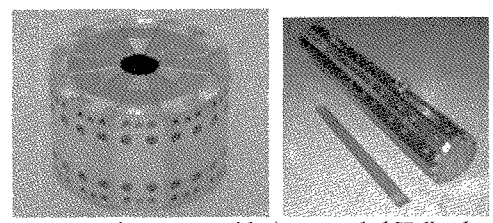

Fig.8. Sextupole magnet with the extended Halbach-type pole configuration for neutron beam focus (left) and quadrupole magnet with the Halbach-type pole configuration for the neutron beam polarizer (right). The aperture of the sextupole is 25mm in diameter and the field strength corresponds to ω~300 s^{-1}. The aperture of the quadrupole is 5mm in diameter and the field strength corresponds to ω ~1400 s^{-1}.

The sextupole magnet is being applied to expand the accessible q-range of the small angle neutron scattering (SANS) instrument. Figure 9 shows the configuration of SANS[16-21].

The focal condition of neutrons from the pinhole collimator to the detector plane is given as

$$\tan\theta_L = \frac{\theta_{L_1}+\theta_{L_2}}{\theta_{L_1}\theta_{L_2}-1}, \tag{11}$$

where

$$\theta_L = \omega\frac{L}{v_z},\ \theta_{L_1} = \omega\frac{L_1}{v_z},\ \theta_{L_2} = \omega\frac{L_2}{v_z}, \tag{12}$$

and v_z is the neutron velocity along the z-axis. In the

case of conventional SANS geometry, the direct beam image on the detector plane is blurred by penumbra of the double slit collimation, which increases the lower limit of the accessible q-region (q_{min}). In the case of SANS with a focusing device, there is no penumbra on the direct beam image. Thus the q_{min} can be expanded to the limitation of the detector position resolution. In addition, the focusing SANS requires only one collimator and diverging neutrons from the collimator also contribute to the observation of scattering in the sample. Consequently, the small q-region can be measured with a minimum loss of incident beam. Thus, the focusing SANS requires a shorter measurement time to achieve a certain statistical significance compared with the conventional SANS.

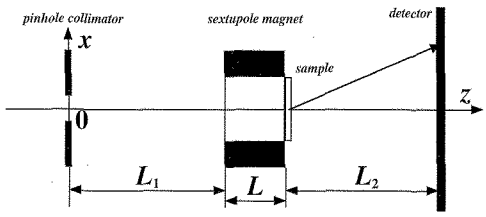

Fig.9. Geometry of the small angle neutron scattering with a focusing device.

The strong spin-selectivity of a quadrupole magnet is suitable for the neutron spin polarizer. We show the neutron polarization P upon transmission through multipole magnets as a function of the normalized time $\theta=\omega t$, assuming the inner surface of the aperture is completely absorptive and the adiabatic spin transport is complete in the aperture. The neutron polarization approaches to unity most rapidly in the case of the quadrupole magnet (n=1). The neutron trajectory can be exactly calculated within the accuracy of the magnetic field and the incident beam distribution in the phase space. The possible fault in the adiabatic spin transport in the vicinity of the magnet axis can be removed by applying additional solenoid field along the z-axis.

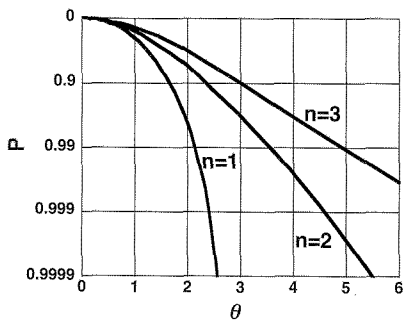

Fig.10. Neutron polarization upon transmission through a quadrupole magnet (n=1), sextupole magnet (n=2) and octapole magnet (n=3) calculated as a function of the normalized time $\theta=\omega t$, assuming the inner surface of the aperture is completely absorptive and the adiabatic spin transport is complete. The vertical axis is measured in the logarithm of 1-P.

4. DISCUSSION

Finally, we try to visualize the bending powers of reflective optical devices, compound refractive and magnetic ones by comparing the curvature of neutron trajectory K and the effective aperture x_c as shown in Fig.10. We define the geometrical aperture as the effective aperture for compound refractive optics and magnetic optics. In the case of reflective optics, we assume the parallel beam is incident on a circularly curved supermirror and bent according to the multiple reflection. We define the effective aperture as the maximum displacement from the mirror surface denoted by x_c. We assume the reflectivity on the surface is 100% in this calculation. Figure 11 shows the reachable regions on the parameter plane of x_c and K.

We point out characteristics of each optics.

(1) Reflective optics is free from strong wavelength dependence and applicable to the polychromatic beam.

(2) Compound refractive optics has the strongest bending power per unit length. The rectangular region of the compound refractive optics can be expanded to larger K by thinning the microprism pieces. We must accept significant scattering neutrons from a large amount of materials on the beam path.

(3) Magnetic optics is relatively weak optics. The neutron trajectory can be precisely calculated within the field accuracy if the incident beam distribution in the phase space is sufficiently well known.

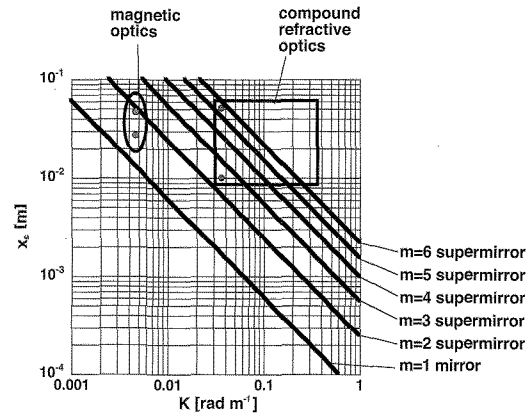

Fig.11. Reachable regions with existing technologies in reflective, compound refractive and magnetic optics on the parameter plane of the effective aperture x_c and the neutron trajectory curvature K.

We surveyed current situation of neutron optics components, which may be applicable for focusing and bending the neutron beam. Possible applications to neutron reflectometry are (1) to bend and adjust the neutron beam to illuminate the horizontal surface of samples, (2) to focus the neutron beam into a small region on the sample surface and (3) to improve the angular resolution by focusing the neutron beam on the detector plane. More detailed discussions on the matching between the technical possibilities and the experimental sensitivity for improving the scientific outputs are valuable to extend the capability of neutron reflectometry.

[1] http://neutrons.ornl.gov/, http://www.j-parc.jp/.
[2] ILL News, No.31, 1999.
[3] M.Hino et al., Nucl. Instrum. Methods A529 (2004) 54.

[4] M.Hino et al., Physica B 385-386 (2006) 1187.
[5] G.E.Ice et al., Nucl. Instrum. Methods A539 (2005) 312.
[6] K.Ikeda et al., Nucl. Instrum. Methods A529 (2004) 78.
[7] M.R.Eskildsen et al., Nature 391 (1998) 563.
[8] S.-M.Choi et al., J. Appl. Cryst. 33 (2000) 793.
[9] T.Adachi et al., Nucl. Instrum. Methods A529 (2004) 112.
[10] T.Shinohara et al., Physica B 385-386 (2006) 1232.
[11] H.M.Shimizu et al., Nucl. Instrum. Methods A430 (1999) 423.
[12] H.M.Shimizu et al., Physica B 385-386 (2006) 989.
[13] J.Suzuki et al., J. Appl. Cryst. 36 (2003) 795.
[14] T.Oku et al.,Physica B 385-386 (2006) 1215.
[15] T.Oku et al., Physica B 387 (2007) 188.
[16] H.M.Shimizu et al., Nucl. Instrum. Methods A529 (2004) 5.
[17] E.Kentzinger et al., Physica B 350 (2004) e779.
[18] S.Okabe et al., J. Appl. Cryst. 38 (2005) 517.
[19] S.Koizumi et al., J. Appl. Cryst. 40 (2007) s474.
[20] T.Oku et al., J. Appl. Cryst. 40 (2007) s408.
[21] H.M.Shimizu et al., Physica B 356 (2005) 121.

(Recieved December 10, 2007 ; Accepted June 14, 2008)